

Synthesis of Novel Curcumin Analogues and Their Evaluation as Selective Cyclooxygenase-1 (COX-1) Inhibitors

Norbert HANDLER,^a Walter JAEGER,^b Helmut PUSCHACHER,^a Klaus LEISSER,^a and Thomas ERKER^{*,a}

^aDepartment of Medicinal Chemistry, University of Vienna; and ^bDepartment of Clinical Pharmacy and Diagnostics, University of Vienna; Althanstrasse 14, A-1090 Vienna, Austria. Received July 26, 2006; accepted October 23, 2006

Curcumin, a major yellow pigment and active component of turmeric, has been shown to possess anti-inflammatory and anti-cancer activities. Recent studies have indicated that cyclooxygenase-1 (COX-1) plays an important role in inflammation and carcinogenesis. In order to find more selective COX-1 inhibitors a series of novel curcumin derivatives was synthesized and evaluated for their ability to inhibit this enzyme using *in vitro* inhibition assays for COX-1 and COX-2 by measuring PGE₂ production. All curcumin analogues showed a higher rate of COX-1 inhibition. The most potent curcumin compounds were (1*E*,6*E*)-1,7-di-(2,3,4-trimethoxyphenyl)-1,6-heptadien-3,5-dione (4) (COX-1: IC₅₀=0.06 μM, COX-2: IC₅₀>100 μM, selectivity index>1666) and (1*E*,6*E*)-methyl 4-[7-(4-methoxycarbonyl)phenyl]-3,5-dioxo-1,6-heptadienyl]benzoate (6) (COX-1: IC₅₀=0.05 μM, COX-2: IC₅₀>100 μM, selectivity index>2000). Curcumin analogues therefore represent a novel class of highly selective COX-1 inhibitors and promising candidates for *in vivo* studies.

Key words curcumin; cancer; cyclooxygenase-1; cyclooxygenase-2

Curcumin (diferuloyl methane, Chart 1) is a major constituent found in the spice turmeric, which is a dried powder from the rhizomes of *Curcuma longa* L. Several *in vitro* and *in vivo* studies demonstrated suppression, retardation, or inversion of carcinogenesis.^{1–3} Furthermore, it also exhibits anti-inflammatory, antioxidant, antiviral, and anti-infectious activities and wound healing properties.^{4–8} Inhibition of arachidonic acid metabolism by curcumin has been suggested to be a key mechanism for its anticarcinogenic action. The enzyme cyclooxygenase (COX) catalyzes the first two steps in the biosynthesis of prostaglandins (PGs) from the substrate arachidonic acid. At least two forms of this enzyme exist.^{9,10}

One of these forms, COX-1, is constitutively expressed and is responsible for maintaining normal physiologic function and the PGs produced by this enzyme play a protective role. The other known form of the enzyme, cyclooxygenase-2 (COX-2), is an inducible form and its expression is affected by various stimuli such as mitogens, oncogenes, tumor promoters, and growth factors.¹⁰ COX-2 has been detected in various tumors and its role in carcinogenesis and angiogenesis has been well documented. Therefore, COX-2 is thought to be a promising therapeutic target for cancer. However, current clinical studies of a COX-2-selective inhibitor, rofecoxib (Vioxx), for preventing recurrence of colorectal polyps in patients with a history of colorectal adenomas were

discontinued and the drug was withdrawn from the market because its use was associated with an increased incidence of cardiovascular events, such as heart attack and stroke.¹¹

Very recently, experimental results have also indicated a possible involvement of the other isoform of COX, COX-1, in angiogenesis, thereby providing the rationale for the development of selective COX-1 inhibitors.^{12,13} These data were also confirmed by *in vitro* studies in isolated ovine COX-1 and COX-2 enzymes which showed that curcumin and its analogues tetrahydrocurcumin and trimethoxydibenzoyl-methane had significantly higher inhibitory effects on the peroxidase activity of COX-1 than that of COX-2.² Furthermore, a recent report by Gupta *et al.*¹⁴ has also indicated that COX-1 is overexpressed in a significant number of ovarian cancers. We therefore investigated whether novel curcumin analogues might achieve an even better and more selective COX-1 inhibition than curcumin. Thus, seven analogues of curcumin were synthesized using standard chemical methods. Each analogue (except the intermediate **2**) was then tested for COX-1 and COX-2 inhibition in an *in vitro* model and the resulting inhibition values compared with that of the clinically established selective COX-2 inhibitor celecoxib. Also molecular docking studies were performed to investigate the ligand-protein interactions responsible for the biological data found.

Results and Discussion

The chemical synthesis of the curcumin analogues was carried out following two known pathways. Their basic principle is the same, but they differ in technique, reaction time and temperature. Generally, the first step was the reaction of acetylacetone with boron oxide building a boron complex, which inhibited an unpleased Knoevenagel reaction. After addition of a corresponding benzaldehyde and a base, the condensation of the acetylacetone–boron complex with the aldehyde and an additional elimination occurred; eventual heating with dilute acid cleaved the boron complex to give the desired curcumin analogues (Chart 2).

Method 1, described by Mazumder *et al.*¹⁵ was successful

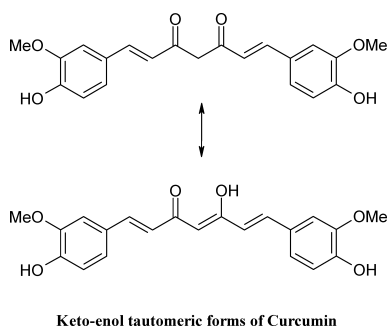


Chart 1. Two Tautomeric Forms of Curcumin

* To whom correspondence should be addressed. e-mail: thomas.erker@univie.ac.at

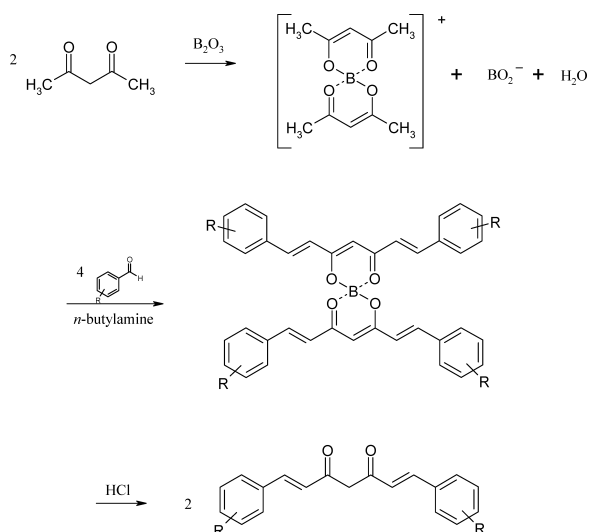
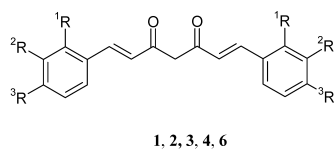


Chart 2. Basic Steps of the Synthesis of Curcuminoids



Compound	¹ R	² R	³ R
1	-H	-F	-F
2	-H	-H	-SCH ₃
3	-H	-H	-SO ₂ -CH ₃
4	-OCH ₃	-OCH ₃	-OCH ₃
6	-H	-H	-COOCH ₃

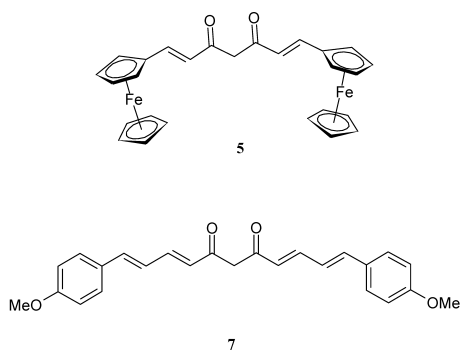


Chart 3. Novel Curcumin Analogues 1—7

in poor yields for compounds **2** and **7**. Method 2, first described by Pabon,¹⁶⁾ was used for the other molecules ending up in poor yields, too. Study of the literature concerning the synthesis of curcuminoids pointed out difficulties, since only some derivatives seemed to be accessible quite well. The yields ranged from about 50% shown only for methoxy-derivatives to poor yields for *p*-(dimethylamino) (36%) or *o*-furyl derivatives (8%), respectively,^{15,16)} and so we tried to improve our pathways. Exact analysis of our syntheses revealed that the volume of *n*-butylamine plays an important role in this kind of reaction and thus, in case of molecules **1** and **4**, its quantity was reduced to obtain the desired compounds in a somehow acceptable yield.

Inhibition of COX-1 and COX-2 by curcumin analogues

Table 1. Inhibitory Effect of 1—7, Curcumin and the Reference Compound Celecoxib on COX-1 and COX-2 Activity (Values Given in μM)

Compound	IC ₅₀ (COX-1)	IC ₅₀ (COX-2)	IC ₅₀ (COX-1)/ IC ₅₀ (COX-2)	IC ₅₀ (COX-2)/ IC ₅₀ (COX-1)
1	0.33	12.58	0.026	38
2	n.d.	n.d.	n.d.	n.d.
3	2.68	>100	<0.026	>37
4	0.06	>100	<0.0006	>1666
5	0.37	9.92	0.037	27
6	0.05	>100	<0.0005	>2000
7	1.14	5.13	0.22	4.5
Curcumin ²⁾	50	>100	0.5	2
Celecoxib	13.7	0.03	456.6	0.002
Indomethacin ²¹⁾	0.018	0.026	0.692	1.444

was then analyzed in a cell-free immunoassay system. Purified ovine enzyme served as the source of COX-1, while the human recombinant enzyme formed the source of COX-2. The inhibition of COX-1 by curcumin analogues (compound **2**, an intermediate, was not tested) is shown in Table 1. All compounds tested demonstrated a several-fold higher inhibitory activity than curcumin itself (COX-1: IC₅₀ = 50 μM , COX-2: IC₅₀ > 100 μM).²⁾

In detail, the results showed that all our curcumin derivatives had a preference towards COX-1 isoenzyme not depending on the substituent of the molecule. Even compound **3** bearing a methylsulfonyl group, which can be found in some COX-2-selective compounds, exhibited an distinct affinity towards COX-1. Nurfina *et al.*⁷⁾ postulated that, besides olefinic double bonds, a 4-hydroxyl group at the phenyl ring of curcuminoids was essential for an antiinflammatory effect. Also position 3 of the aromatic ring played an important role for the pharmacological profile, since bigger 3-alkyl groups (like *tert*-butyl) lead to inactive molecules, whereas lower alkyl and especially 3,5-dialkyl-substituents showed high oedema inhibiting activity. Selvam *et al.*¹⁷⁾ calculated docking studies with curcumin and some derivatives, which revealed that these compounds could dock into the active site of only COX-1. In case of the COX-2 enzyme complex only curcumin itself interacted with the enzyme, but no hydrogen bonding interactions were detected for the other molecules. Thus we chose derivatives without hydroxy groups but lipophilic and mainly polar groups to check possible SAR concerning COX-1 interaction.

The data are presented in this paper (Table 1), where all novel curcumin derivatives showed a distinct affinity towards COX-1 isoenzyme. The corresponding IC₅₀ values reached from 2.68 μM (compound **3**) to 0.05 μM (compound **6**) including selectivity indices (IC₅₀(COX-2)/IC₅₀(COX-1)) from 4.5 for compound **7** to >2000 for compound **6**. Especially the trimethoxy derivative **4** as well as the methyl ester **6** exhibited very pronounced and selective COX-1 inhibition (IC₅₀ = 0.06 and 0.05 μM , selectivity indices >1666 and >2000), whereas the other molecules showed just poor affinities and selectivities towards this isoenzyme. However, also compound **3**, bearing a methylsulfonyl group, a group found in some COX-2 inhibiting molecules, had weak effects on COX-1 but almost none towards COX-2 (IC₅₀(COX-1) = 2.68 μM , IC₅₀(COX-2) > 100 μM , selectivity index >37). The other molecules exhibited only little COX-1-effects and selectivities with IC₅₀ values ranging from 0.33 to 2.68 μM

and selectivity indices from 4.5 to 38, respectively.

In order to better understand the anti-inflammatory activities of compounds **1**, **3**, **4**, **6** and **7** we performed a molecular docking analysis. We tried to understand the ligand-protein interaction responsible for the perceived COX-1/COX-2 inhibitory data. Docking conformations of compounds **1**, **3**, **4**, **6** and **7** were created by a systematic conformational search with the MMFF94x as implemented in MOE. Each rotatable bond of the heptanoid part of the compounds was assigned a 60° rotation increment. Rotatable bonds of substituents of the phenyl rings were assigned a 30° rotation increment. All resulting conformers were subjected to full energy minimization using the MMFF94x force field to a gradient of 0.05 kcal/mol. Conformers having an energy of 15 kcal/mol above the lowest energy found were not taken into consideration. Duplicate entries in the resulting conformer database were discarded using a RMS filter of 0.1 Å. This resulted in databases of 3000 conformers on average. From these databases 1500 conformers were selected based on the dissimilarity of their internal coordinates. The resulting conformer databases were used as starting structures for a rigid docking simulation. We used the simple grid energy scoring function to score the docked conformations as implemented in program Dock 6.0. Partial charges were calculated semi-empirically using the AM1 hamiltonian. From the docked conformations only the best scored conformation was retained. The complexes were subsequently energy minimized using force field MMFF94 to a gradient of 0.05 kcal/mol and were rescored using the same grid. All compounds could be docked into the active site of 1PGG successfully. The individual grid scores are shown in Table 2. All compounds showed hydrogen bond interaction to the 1PGG protein. The exact numbers of hydrogen bonds can be seen in Table 3.

The active site of 1PGG is considered to be constituted of the amino acid residues ARG120, SER530, TYR385 and GLU524.¹⁸⁾ **1**, **6** and **7** exhibited a very good DOCK 6.0 grid score showing favorable van der Waals interactions. Compound **1** showed two hydrogen bonds. The two carbonyl oxygens were acceptors for hydrogen bonds forming from ARG83 (NH1). The O–N distance was found to be 3.09 and 2.51 Å; the O–H distance was found to be 2.38 and 1.52 Å, respectively (Fig. 1). Although compound **3** and **4** exhibited only moderate to weak interactions calculated with DOCK, they show a tight hydrogen bond network. **3** is able to build three hydrogen bonds to 1PGG. These hydrogen bonds are formed by ARG83 and the sulfonyl oxygen of **3** with a bond length of 1.52 Å, ARG120 NH1 and the carbonyl oxygen of **3** with a bond length of 1.51 and ARG120 NH2 and the car-

Table 2. Total Grid Score of Compounds Interacting with 1PGG

Compound	Grid score (Dock 6.0) 1PGG
1	-24.60
3	-16.09
4	-11.33
6	-20.10
7	-24.46

Table 3. Hydrogen Bond Interaction with 1PGG

Compound	No. of hydrogen bonds	Bond lengths [Å]
1	2	2.38, 1.52
3	3	1.52, 1.51, 2.32
4	3	1.59, 1.43, 1.80
6	2	1.52, 2.38
7	4	1.33, 1.47, 1.86, 1.99

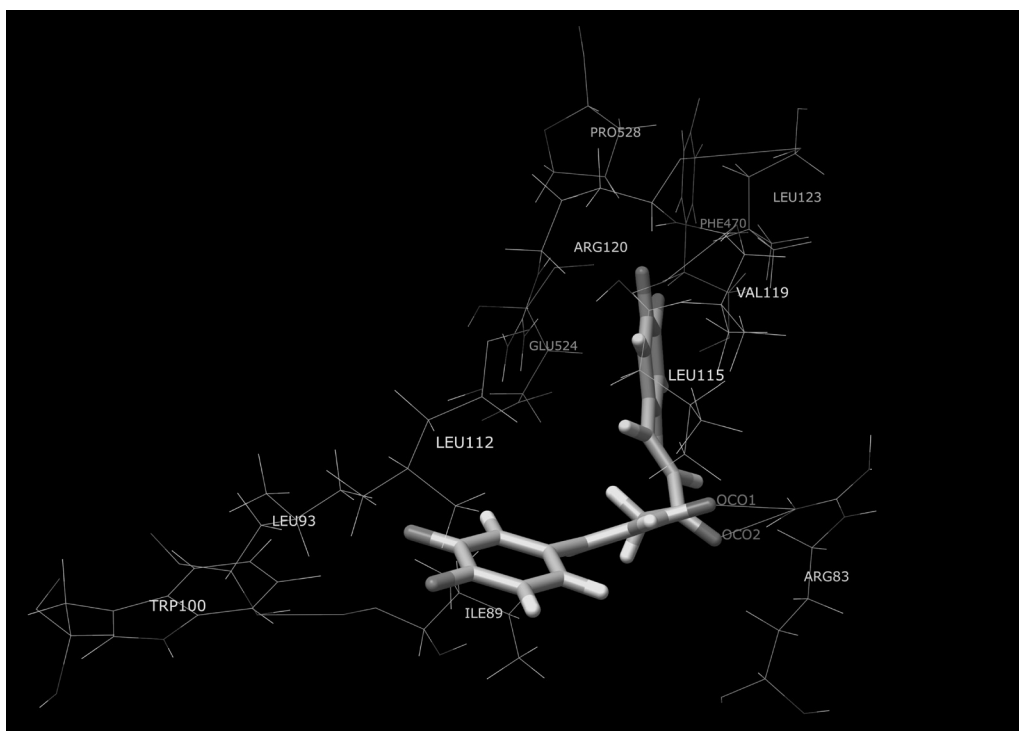


Fig. 1. Binding of **1** into the Active Site of 1PGG

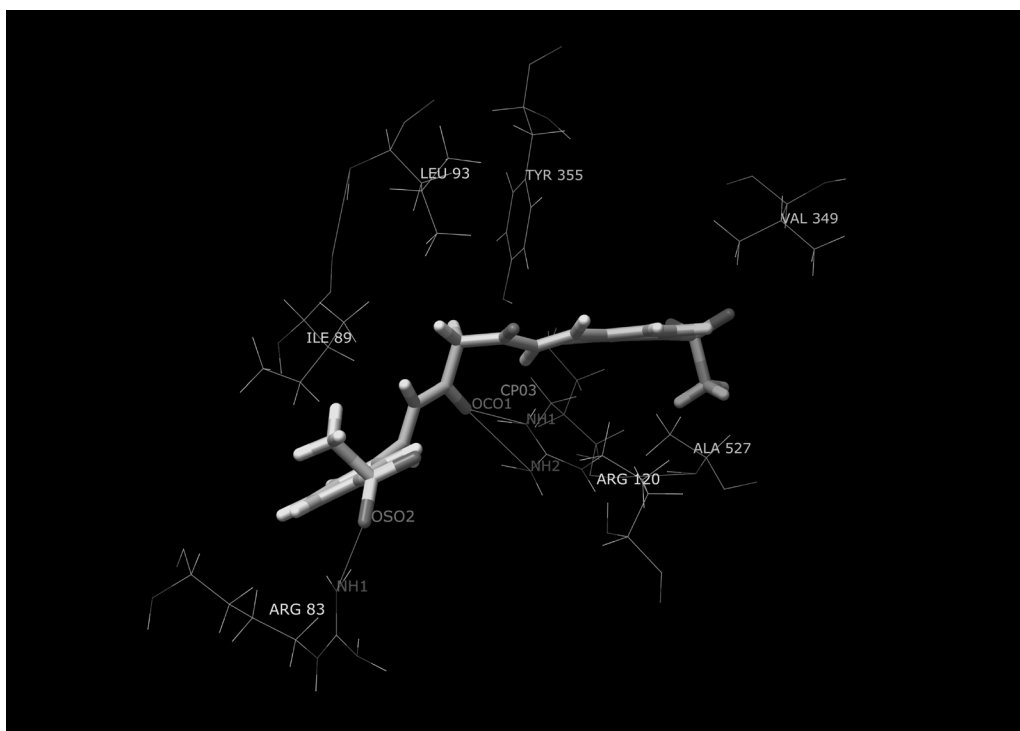


Fig. 2. Binding of **3** into Active Site of 1PGG

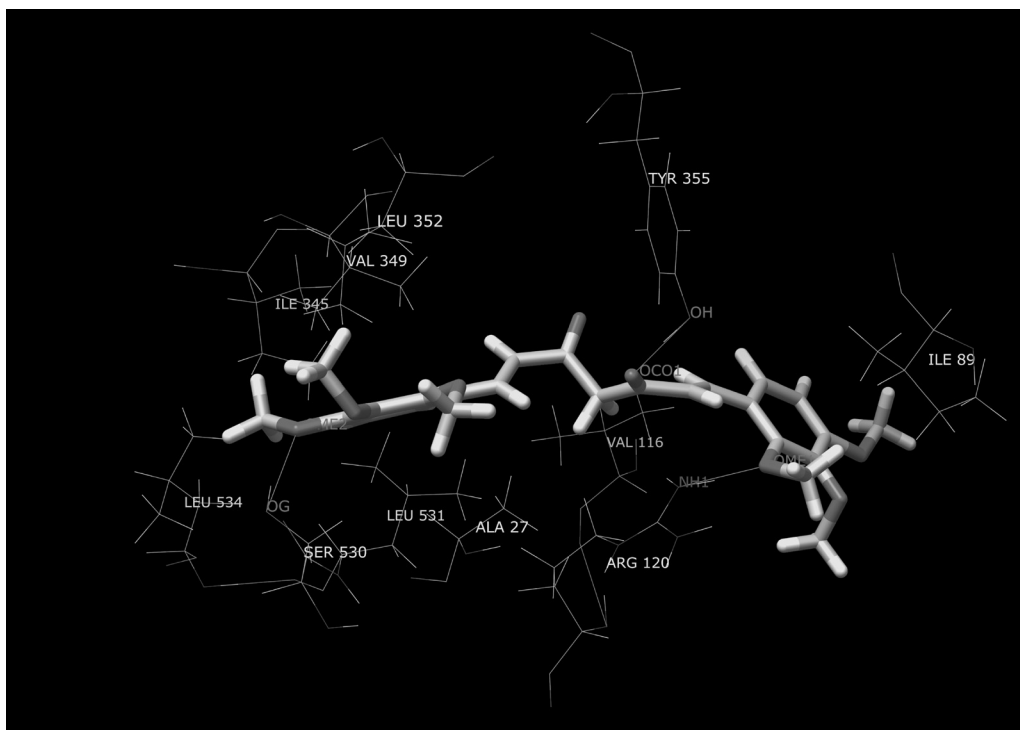


Fig. 3. Binding of **4** into the Active Site of 1PGG

bonyl oxygen of **3** with a bond length of 2.32, respectively (Fig. 2).

Compound **4** exhibited three hydrogen bonds to the 1PGG protein. These hydrogen bonds were formed by ARG120 and the methoxy group of **4**, TYR355 and the carbonyl oxygen of **4** and SER530 and the second methoxy group of **4**. The calculated bond length were 1.59 Å, 1.43 Å and 1.79 Å respec-

tively (Fig. 3). We think that this accounts for the low observed IC_{50} of compound **4**. Compound **6** showed an excellent electrostatic and steric interaction with 1PGG and could build two hydrogen bonds with 1PGG (Fig. 4). These were formed by TYR355 and one of the carbonyl oxygens and SER530 and the other carbonyl oxygen of the heptanoid part of **6**. The bond length were 1.53 Å and 2.38 Å respectively.

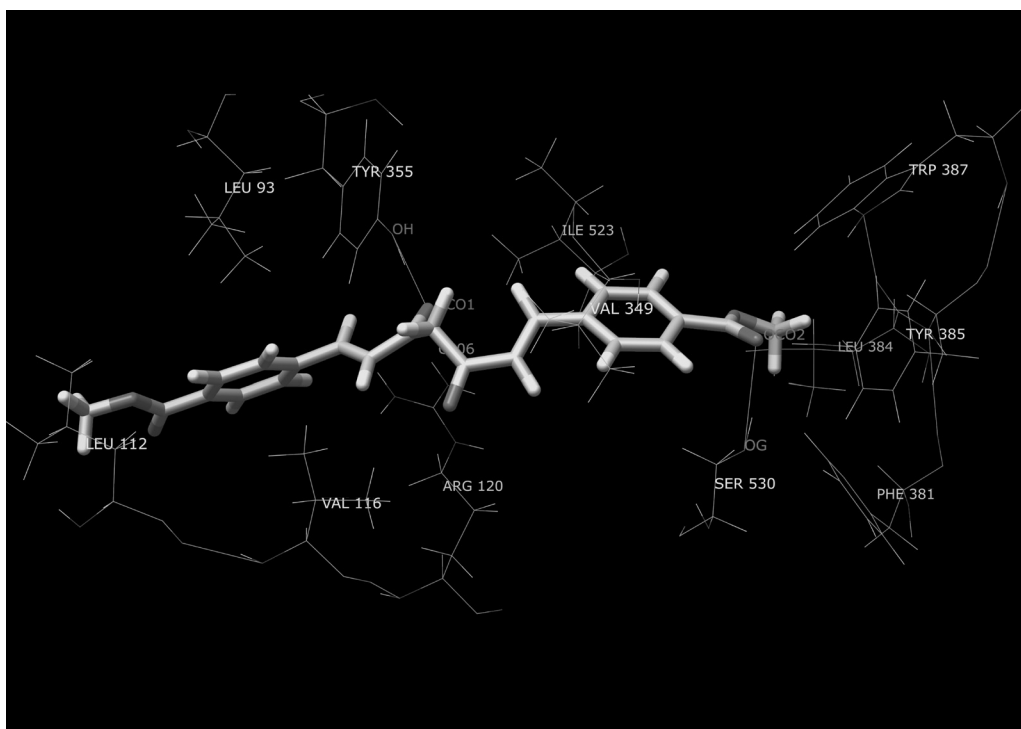


Fig. 4. Binding of 6 into the Active Site of 1PGG

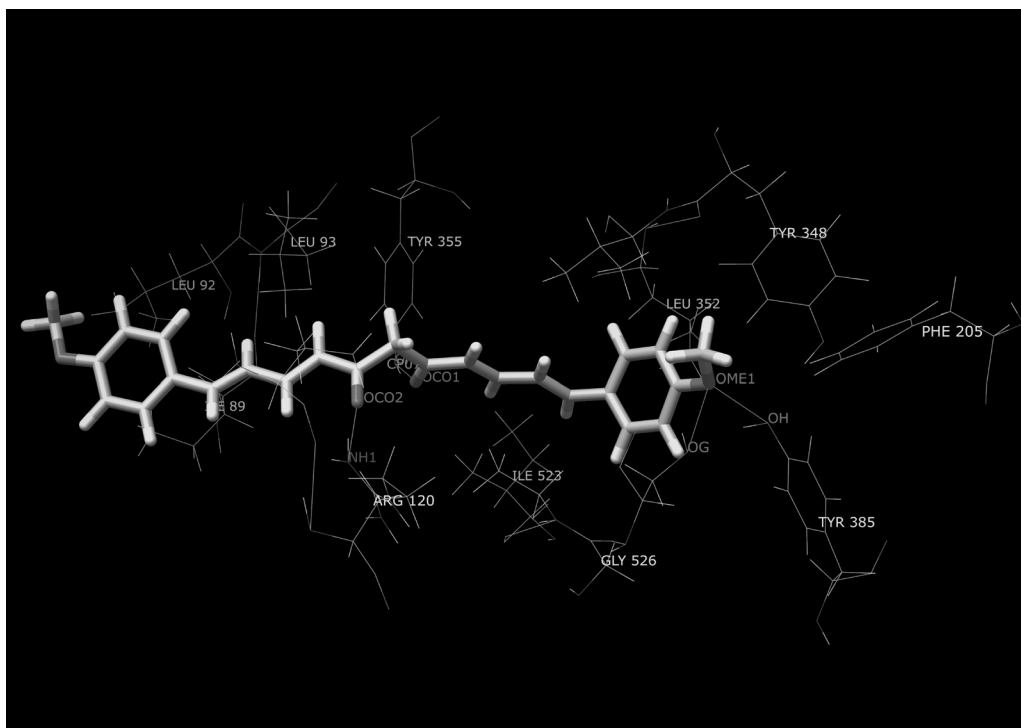


Fig. 5. Binding of 7 into the Active Site of 1PGG

Four hydrogen bonds were formed by compound 7 (Fig. 5). Three hydrogen bonds were formed with amino acids of the active site of 1PGG ARG120, TYR385 and SER530. One hydrogen bond was formed with TYR355. The hydrogen bond lengths were 1.24 Å, 1.86 Å, 1.99 Å and 1.47 Å respectively.

All five compounds used for docking showed a good van

der Waals interaction with 1PGG. One of the phenyl rings of compound 1 was surrounded by GLU524, ARG120 and PHE470. The heptanoid part of 1 was surrounded by ILE89, ILE115 and VAL119. The second phenyl ring was surrounded by LEU93, TRP100 and LEU112. The deeper buried phenyl ring of compound 3 is surrounded by the active site amino acid residues SER530, TYR385, LEU352 and

Table 4. Total Grid Score of Compounds Interacting with 4COX

Compound	Grid score (Dock 6.0) 4COX
1	-16.32
3	-46.76
4	n.d.
6	-36.02
7	-35.99
Indomethacin	-45.89

Table 5. Hydrogen Bond Interaction with 4COX

Compound	No. of hydrogen bonds	Bond lengths [Å]
1	2	1.46, 3.00
3	2	2.07, 1.64
4	n.d.	n.d.
6	2	1.49, 1.65
7	3	1.54, 1.65, 2.15
Indomethacin	3	1.33, 2.46, 2.26

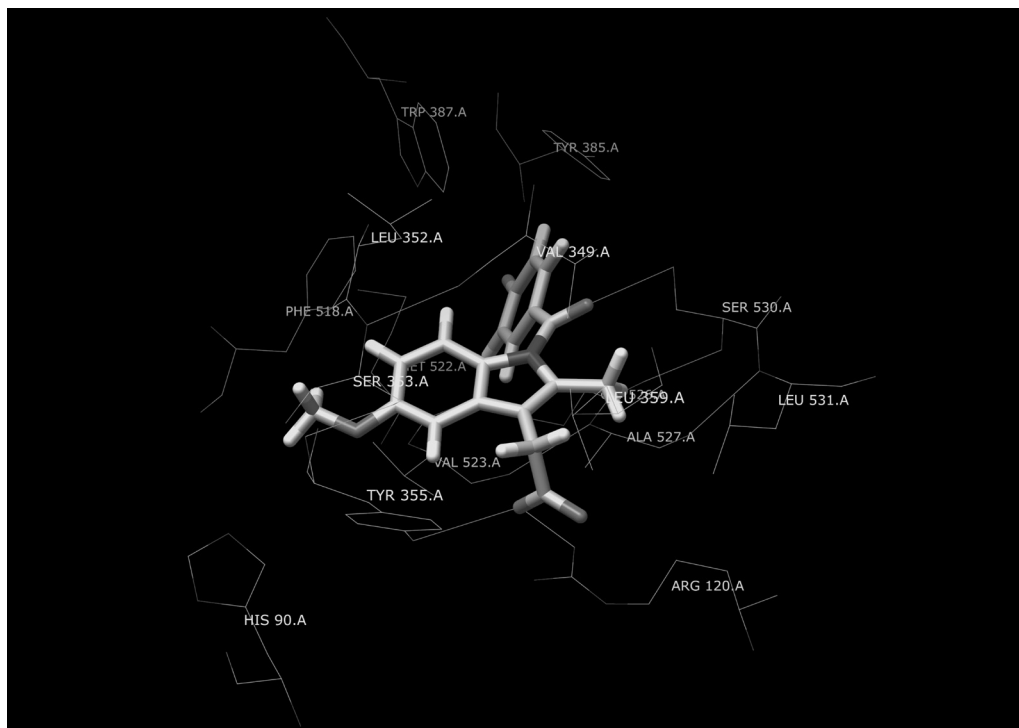


Fig. 6. Interaction of Indomethacin with 4COX

ILE523. The heptanoid part of **3** was surrounded by GLU524, ARG120 and VAL116; the second ring of **3** was surrounded by ILE89 and ARG83. Similar trends were observed for the other compounds under investigation.

After docking simulations with 1PGG (COX-1) we tried to dock the compounds considered in the first simulation into the active site of 4COX (COX-2). The active site of 4COX is considered to be formed of the amino acid residues TYR385, that is supposed to abstract one hydrogen from the substrate, SER530, which is acetylated by acetylsalicylic acid and HEME.¹⁹⁾ All compounds except **4** could be docked into the active site of 4COX with a reasonable steric and electrostatic interaction. As a test compound, we docked the co-crystallized ligand indomethacin into the active site of 4COX. The results can be seen in Table 4. Indomethacin showed the best electrostatic and steric interaction scores and the tightest hydrogen bond network with the active site (Fig. 6). Indomethacin formed hydrogen bonds between ARG120, TYR355 and SER530 with bond length of 1.33, 2.46 and 2.26 respectively.

The hydrogen bonds formed by the curcumin analogues complexes considered in this work and 4COX were much longer than those of the respective 1PGG complexes (Table 5 and Fig. 7). We therefore argue, that this is the reason for the

selectivity of the compounds under investigation.

In conclusion, we have demonstrated that our curcumin analogues were selective COX-1 inhibitors with submicromolar to micromolar IC₅₀ values and promising selectivities. Especially lipophilic and polar substituents on the phenyl ring, like methoxy or methyl ester groups improved the specificity of the compounds. The biological data were also confirmed by docking studies which revealed good van der Waals interaction and hydrogen bonding towards COX-1 isoenzym performed by our curcuminoid molecules. As this isoform is overexpressed in a significant number of cancer cells and tissues our present results may yield in new candidate drugs for the treatment of these tumor entities.

Experimental

Chemistry Melting points were determined on a Kofler hot stage apparatus and are uncorrected. The ¹H- and ¹³C-NMR spectra were recorded on a Varian UnityPlus-200 (200 MHz). Chemical shifts are reported in δ values (ppm) relative to Me₄Si line as internal standard and *J* values are reported in Hertz. Mass spectra were obtained by a Shimadzu GC/MS QP 1000 EX using EI method. The elemental analysis obtained were within ±0.4% of the theoretical values for the formulas given.

The following compounds were synthesized *via* two different pathways.

Method 1¹⁵⁾: In a dry three-necked flask acetylacetone (5 mmol, 0.51 ml) and boron oxide (3.5 mmol, 0.244 g) were solved in absolute ethyl acetate and stirred for 30 min at 40 °C. Then the corresponding aldehyde (10 mmol)

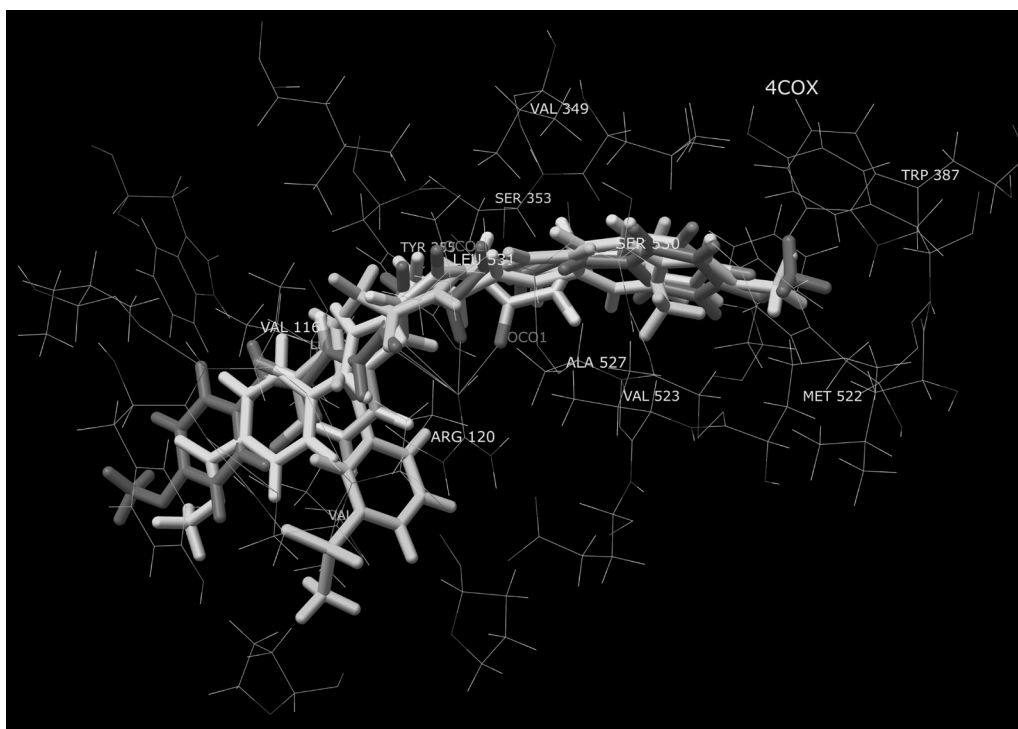


Fig. 7. Interaction of **1**, **3**, **6** and **7** with 4COX

and tributyl borate (10 mmol, 2.4 ml) were added and stirred for another 30 min. *N*-Butylamine (quantities given below) was solved in dry ethyl acetate and then added over a period of 15 min. The mixture was heated to 40 °C for 24 h. Then 5 ml of HCl (10%) were added and heated to 60 °C for an additional hour. The aqueous phase was extracted with ethyl acetate several times, the organic layers were dried over Na₂SO₄ and the solvent distilled off. An unsoluble precipitate (part of the product) was filtered off and recrystallized with the residue from various solvents.

Method 2¹⁶⁾: In a dry three-necked flask acetylacetone (5 mmol, 0.51 ml) and boron oxide (3.5 mmol, 0.244 g) were solved in 5 ml absolute ethyl acetate and heated to 75 °C for 1 h. The corresponding benzaldehyde (10 mmol) and tributyl borate (10 mmol, 2.4 ml) were mixed with ethyl acetate, stirred for 45 min and then added to the solution. The mixture was heated to 100 °C for 1 h. Then *n*-butylamine (quantities given below) was solved in 5 ml ethyl acetate and 3.85 ml of this solution were added drop-by-drop over a period of 90 min. The reaction was stirred for 18 h at 85 °C and then cooled to 60 °C. Then 5 ml of a HCl solution (10%) were heated to 50 °C, added and the mixture was stirred at 60 °C for 1 h. The solution was extracted three times with ethyl acetate, the organic layers were dried over Na₂SO₄ and the solvent reduced to 7–8 ml. Two and a half milliliters ethanol were added, the solution was cooled overnight, then the precipitate was filtered off and recrystallized to obtain the purified product.

(1E,6E)-1,7-Di-(3,4-difluorophenyl)-1,6-heptadien-3,5-dione (1) The compound was synthesized from 3,4-difluorobenzaldehyde (10 mmol, 1.16 ml) and *n*-butylamine (2.5 mmol, 0.25 ml) following method 2. Crystallization from ethyl acetate/water (1+1) afforded 0.066 g (3.8%) of a yellow solid; mp 137 °C. ¹H-NMR (CDCl₃) δ: 5.82 (1H, s), 6.52 (2H, d, *J*_E=15.8 Hz), 7.12–7.42 (6H, m), 7.56 (2H, d, *J*_E=15.8 Hz), 15.76 (1H, br s). ¹³C-NMR (CDCl₃) δ: 102.2, 116.1 (d, *J*_{C,F}=18.0 Hz), 117.9 (d, *J*_{C,F}=18.0 Hz), 124.9 (quintet), 132.1 (quartet), 138.3–138.5 (m), 148.5 (d, *J*_{C,F}=22.2 Hz), 153.6 (d, *J*_{C,F}=39.4 Hz), 182.8; MS (EI) *m/z*: 348 (M⁺), 306, 167, 139, 119. *Anal.* Calcd for C₁₉H₁₂O₂F₄: C, 65.52; H, 3.47. Found: C, 65.41; H, 3.69.

(1E,6E)-1,7-Di-[4-(methylmercapto)phenyl]-1,6-heptadien-3,5-dione (2) The compound was synthesized from 4-(methylmercapto)benzaldehyde (10 mmol, 1.33 ml) and *n*-butylamine (7.5 mmol, 0.74 ml) following method 1. Crystallization from ethanol afforded 1.14 g (62%) of a yellow solid; mp 194 °C. ¹H-NMR (CDCl₃) δ: 2.51 (6H, s), 5.81 (1H, s), 6.58 (2H, d, *J*_E=15.8 Hz), 7.24 (4H, A-part of AB-system, *J*_{A,B}=8.7 Hz), 7.47 (4H, B-part of AB-system, *J*_{A,B}=8.7 Hz), 7.62 (2H, d, *J*_E=15.8 Hz), enol OH signal not detected; ¹³C-NMR (CDCl₃) δ: 15.2, 101.8, 123.1, 126.0, 128.5, 140.0,

183.2. MS (EI) *m/z*: 368 (M⁺), 279, 201, 105, 77. *Anal.* Calcd for C₂₁H₂₀O₂S₂: C, 68.45; H, 5.47. Found: C, 68.20; H, 5.25.

(1E,6E)-1,7-Di-[4-(methylsulfonyl)phenyl]-1,6-heptadien-3,5-dione (3) (1E,6E)-1,7-Di-[4-(methylmercapto)phenyl]-1,6-heptadien-3,5-dione (**2**) (2.5 mmol, 0.924 g) was solved in acetone; then oxone[®] (10 mmol, 6.14 g) in 15 ml water was added and the mixture was stirred at room temperature for 24 h. After addition of 20 ml ammonia (10%) and stirring for an additional hour water was added, the precipitate formed was filtered off and washed with water. The yellow solid was solved in DMF and ethanol was added to isolate 0.278 g (25%) of the pure compound; mp >300 °C. ¹H-NMR (DMSO-*d*₆) δ: 3.24 (6H, s), 5.77 (1H, s), 7.02 (2H, d, *J*_E=15.7 Hz), 7.48 (2H, d, *J*_E=15.7 Hz), 7.87–7.98 (8H, m), OH signal not detected; ¹³C-NMR (DMSO-*d*₆) δ: 43.7, 104.6, 127.7, 128.4, 134.3, 134.4, 140.6, 141.0, 181.1. MS (EI) *m/z*: 432 (M⁺), 201, 111, 68. *Anal.* Calcd for C₂₁H₂₀O₆S₂: C, 58.32; H, 4.66. Found: C, 58.47; H, 4.34.

(1E,6E)-1,7-Di-(2,3,4-trimethoxyphenyl)-1,6-heptadien-3,5-dione (4) The compound was synthesized from 2,3,4-trimethoxybenzaldehyde (10 mmol, 1.96 g) and *n*-butylamine (2.5 mmol, 0.25 ml) following method 2. Purification was carried out with column chromatography (eluent toluene/ethyl acetate 8+2) and crystallization from ethanol (80%) to afford 0.087 g (3.8%) of a yellow solid; mp 115 °C. ¹H-NMR (DMSO-*d*₆) δ: 3.89 (6H, s), 3.91 (6H, s), 3.94 (6H, s), 5.83 (1H, s), 6.63 (2H, d, *J*_E=15.0 Hz), 6.71 (2H, A-part of AB-system, *J*_{A,B}=8.8 Hz), 7.30 (2H, B-part of AB-system, *J*_{A,B}=8.8 Hz), 7.85 (2H, d, *J*_E=15.8 Hz), 16.06 (1H, br s). ¹³C-NMR (DMSO-*d*₆) δ: 56.1, 60.9, 61.4, 101.3, 107.6, 122.2, 123.2, 123.4, 135.3, 142.4, 153.4, 155.4, 183.6. MS (EI) *m/z*: 278 (half mass), 247, 235, 204, 131, 43. *Anal.* Calcd for C₂₅H₂₈O₈: C, 65.78; H, 6.18. Found: C, 65.49; H, 6.17.

(1E,6E)-1,7-Diferrocenyl-1,6-heptadien-3,5-dione (5) The compound was synthesized from ferrocenealdehyde (10 mmol, 2.18 g) and *n*-butylamine (7.5 mmol, 0.74 ml) following method 2. Crystallization from ethyl acetate afforded 0.205 g (8.3%) of a purple solid; mp 210 °C. ¹H-NMR (CDCl₃) δ: 4.17 (10H, s), 4.44 (4H, s), 4.52 (4H, s), 5.62 (1H, s), 6.21 (2H, d, *J*_E=15.5 Hz), 7.54 (2H, d, *J*_E=15.5 Hz), enol OH signal not detected. ¹³C-NMR (CDCl₃) δ: 68.5, 69.7, 71.0, 79.7, 100.1, 121.3, 141.5, 182.7. MS (EI) *m/z*: 492 (M⁺), 280, 246, 239, 121, 56. HR-MS *m/z*: 492.0476 (Calcd for C₂₇H₂₄O₂Fe₂: 492.0459).

(1E,6E)-Methyl 4-[7-(4-methoxycarbonyl)phenyl]-3,5-dioxo-1,6-heptadienyl]benzoate (6) The compound was synthesized from (4-formyl)-methylbenzoate (10 mmol, 1.64 g) and *n*-butylamine (7.5 mmol, 0.74 ml) following method 2. Crystallization from ethyl acetate afforded 0.334 g

(16.8%) of a yellow solid; mp 215 °C: ¹H-NMR (CDCl₃) δ: 3.94 (6H, s), 5.90 (1H, s), 6.71 (2H, d, *J*_E=15.9 Hz), 7.62 (4H, A-part of AB-system, *J*_{AB}=8.2 Hz), 7.69 (2H, d, *J*_E=15.9 Hz), 8.07 (4H, B-part of AB-system, *J*_{AB}=8.2 Hz), 15.74 (1H, br s). ¹³C-NMR (CDCl₃) δ: 52.3, 102.5, 126.1, 127.9, 130.1, 131.2, 139.1, 139.4, 166.4, 182.9; MS (EI) *m/z*: 392 (M⁺), 145, 115, 102, 59. *Anal.* Calcd for C₂₃H₂₀O₆: C, 70.40; H, 5.14. Found: C, 70.18; H, 5.04.

(1E,3E,8E,10E)-1,11-Di-(4-methoxyphenyl)-1,3,8,10-undecatetraen-5,7-dione (7) The compound was synthesized from 4-methoxycinnamaldehyde (10 mmol, 1.62 g) and *n*-butylamine (7.5 mmol, 0.74 ml) following method 1. Crystallization from ethanol (70%) afforded 0.219 g (11.3%) of an orange solid; mp 210 °C. ¹H-NMR (CDCl₃) δ: 3.83 (6H, s), 5.66 (1H, s), 6.12 (2H, d, *J*_E=15.0 Hz), 6.72–6.93 (8H, m), 7.36–7.51 (6H, m), 15.90 (1H, br s). ¹³C-NMR (CDCl₃) δ: 55.4, 101.5, 114.3, 125.0, 126.6, 128.7, 129.1, 139.9, 141.1, 160.4, 183.1. MS (EI) *m/z*: 388 (M⁺), 187, 121, 57. *Anal.* Calcd for C₂₅H₂₄O₄·0.25H₂O: C, 76.31; H, 6.29. Found: C, 76.33; H, 6.45.

Cyclooxygenase Assay The effects of the test compounds on COX-1 and COX-2 were determined by measuring prostaglandin E₂ (PGE₂) using a COX Inhibitor Screening Kit (Catalog No 560131) from Cayman Chemicals, Ann Arbor, Michigan, U.S.A. Reaction mixtures were prepared in 100 mM Tris-HCl buffer, pH 8.0 containing 1 μM heme and COX-1 (ovine) or COX-2 (human recombinant) and pre-incubated for 10 min in a waterbath (37 °C). The reaction was initiated by the addition of 10 μl arachidonic acid (final concentration in reaction mixture 100 μM). After 2 min the reaction was terminated by adding 1 M HCl and finally PGE₂ was quantified by an ELISA method. The test compounds were dissolved in DMSO and diluted to the desired concentration with 100 mM potassium phosphate buffer (pH 7.4). Following transfer to a 96 well plate coated with a mouse anti-rabbit IgG, the tracer prostaglandin acetylcholine esterase and primary antibody (mouse anti PGE₂) were added. Plates were then incubated at room temperature overnight, reaction mixtures were removed, and the wells were washed with 10 mM potassium phosphate buffer containing 0.05% Tween 20. Ellman's reagent (200 μl) was added to each well and the plate was incubated at room temperature (exclusion of light) for 60 min, until the control wells yielded an OD=0.3–0.8 at 412 nm. A standard curve with PGE₂ was generated from the same plate, which was used to quantify the PGE₂ levels produced in the presence of test samples. Results were expressed as a percentage relative to a control (solvent-treated samples). All determinations were performed in duplicate and values generally agreed within 10%.

Docking Studies All calculations were performed on a SUN Ultra 40 workstation using program DOCK 6.0 (Kuntz, I.D., DOCK, UCSF Box 2240, UCSF, San Francisco, CA 94143-2240) and MOE (Molecular Operating Environment, Chemical Computing Group Inc., Montreal, Quebec, Canada). The crystal structures of COX-1 and COX-2 co-crystallized with indomethacin (1PGG.pdb and 4COX.pdb respectively)^{19,20} were taken from the Brookhaven Protein Databank¹⁸ and used for docking. Regions with a 7.0 Å radius from the complexed inhibitor were marked as interesting.

References

- Weber W. M., Hunsaker L. A., Roybal C. N., Bobrovnikova-Marjon E. V., Abcouwer S. F., Royer R. E., Deck L. M., Vander Jagt D. L., *Bioorg. Med. Chem.*, **14**, 2450–2461 (2006).
- Hong J., Bose M., Ju J., Ryu J., Chen X., Sang S., Lee M., Yang C., *Carcinogenesis*, **25**, 1671–1679 (2004).
- Woo H. B., Shin W., Lee S., Ahn C. M., *Bioorg. Med. Chem. Lett.*, **15**, 3782–3786 (2005).
- Venkateswarlu S., Ramachandra M. S., Subbaraju G. V., *Bioorg. Med. Chem.*, **13**, 6374–6380 (2005).
- Goel A., Boland C. R., Chauhan D. P., *Cancer Lett.*, **172**, 111–118 (2001).
- Lev-Ari S., Strier L., Kazanov D., Madar-Shapiro L., Dvory-Sobol H., Pinchuk I., Marian B., Lichtenberg D., Arber N., *Clin. Cancer Res.*, **11**, 6738–6744 (2005).
- Nurfina A. N., Reksোধadiprodo M. S., Timmermann H., Jenie U. A., Sugiyanto D., van der Goot H., *Eur. J. Med. Chem.*, **32**, 321–328 (1997).
- Joe B., Vijaykamur N., Lokesh B. R., *Crit. Rev. Food Sci. Nutr.*, **44**, 97–111 (2004).
- Xie W. L., Chipman J. G., Robertson D. L., Erikson R. L., Simmons D. L., *Proc. Natl. Acad. Sci. U.S.A.*, **88**, 2692–2696 (1991).
- Fournier D. B., Gordon G. B., *J. Cell Biochem. Suppl.*, **34**, 97–102 (2000).
- Onn A., Tseng J. E., Herbst R. S., *Clin. Cancer Res.*, **7**, 3311–3313 (2001).
- Kitamura T., Itoh M., Noda T., Matsuura M., Wakabayashi K., *Int. J. Cancer*, **109**, 576–580 (2004).
- Sano H., Noguchi T., Miyajima A., Hashimoto Y., Miyachi H., *Bioorg. Med. Chem. Lett.*, **16**, 3068–3072 (2006).
- Gupta R. A., Tejada L. V., Tong B. J., Das S. K., Morrow J. D., Dey S. K., DuBois R. N., *Cancer Res.*, **63**, 906–911 (2003).
- Mazumder A., Neamati N., Sunder S., Schulz J., Pertz H., Eich E., Pommier Y., *J. Med. Chem.*, **40**, 3057–3063 (1997).
- Pabon H. J. J., *Rec. Trav. Chim. Pays-Bas*, **83**, 379–386 (1964).
- Selvam C., Jachak S. M., Thilagavathi R., Chakraborti A. K., *Bioorg. Med. Chem. Lett.*, **15**, 1793–1797 (2005).
- Abloa E. E., Bernstein F. C., Bryant S. H., Koetzle T. F., Weng J., "Protein Data Bank in Crystallographic Databases-Information Content, Software Systems, Scientific Applications," ed. by Allen F. H., Berjehoff G., Sievers R., Data Commission of the International Union of Crystallography, Bonn, 1987, p. 171.
- Kurumbail R. G., Stevens A. M., Gierse J. K., McDonald J. J., Stegeman R. A., Pak J. Y., Gildehaus D., Miyashiro J. M., Penning T. D., Seibert K., Isakson P. C., Stallings W. C., *Nature (London)*, **384**, 644–648 (1996).
- Loll P. J., Picot D., Ekabo O., Garavito R. M., *Biochemistry*, **35**, 7330–7340 (1996).
- Riendeau D., Percival M. D., Boyce S., Brideau C., Charleson S., Cromlish W., Ethier D., Evans J., Falgoutyret J.-P., Ford-Hutchinson A. W., Gordon R., Greig G., Gresser M., Guay J., Kargman S., Leger S., Mancini J. A., O'Neill G., Ouellet M., Rodger I. W., Therien M., Wang Z., Webb J. K., Wong E., Chan C. C., *Brit. J. Pharmacol.*, **121**, 105–117 (1997).